Thermochimica Acta 515 (2011) 43–50

Contents lists available at ScienceDirect

Thermochimica Acta

journal homepage: www.elsevier.com/locate/tca

Thermal study of low-grade magnesium hydroxide used as fire retardant and in passive fire protection

J. Formosa[a,b], J.M. Chimenos[a,*], A.M. Lacasta[c], L. Haurie[b]

[a] Department of Materials Science and Metallurgical Engineering, University of Barcelona (UB), Martí i Franquès, 1, E-08028 Barcelona, Spain
[b] Department of Architectural Technology II, Technical University of Catalonia (UPC), Avda. Dr. Marañón 44, E-08028 Barcelona, Spain
[c] Department of Applied Physics, Technical University of Catalonia (UPC), Avda. Dr. Marañon 44, E-08028 Barcelona, Spain

ARTICLE INFO

Article history:
Received 21 October 2010
Received in revised form 9 December 2010
Accepted 15 December 2010
Available online 29 December 2010

Keywords:
Magnesium hydroxide
Thermal analysis
Low-grade magnesium hydroxide
Passive fire protection
Direct sulphation

ABSTRACT

Low-grade magnesium hydroxide is being used with very promising results as flame retardant filler in polymeric materials and as aggregate in the formulation of mortars for passive fire protection, combining an economic and sustainable solution. Simultaneous TGA–DSC was used to evaluate low-grade magnesium hydroxide thermal decomposition in order to examine the suitability of this product for a broad range of temperatures. Thermal analysis in air shows an unexpected exothermic peak, as well as the endothermic peaks corresponding to the decomposition of magnesium hydroxide, magnesite and dolomite. Thermal decomposition using nitrogen as gas flow does not show the exothermic peak, whereas a new endothermic peak corresponding to decomposition of calcite appears. *In situ* XRD patterns collected in air atmosphere at high temperature allows determining the presence of anhydrite, which was related to direct sulphation of calcite from the sulphur trioxide generated during the combustion of petcoke adsorbed on the particle surface of the low-grade magnesium hydroxide.

1. Introduction

Magnesium hydroxide is widely used as a flame retardant and smoke-suppressor in polymeric materials [1,2]. Its mechanism of action is based on the heat absorbed from the combustion system when it undergoes its endothermic decomposition with an associated heat of 1.42 mJ kg^{-1} [3]. Furthermore the water vapour released during the decomposition dilutes the combustion gases and the magnesium oxide layer generated during the breakdown could act as a protective char in the condensed phase [4]. Unlike the commonly used aluminium hydroxide (alumina trihydrate, ATH), which starts decomposing around 200 °C, magnesium hydroxide begins to decompose above 300 °C [5,6]. This allows the use of magnesium hydroxide in polymers with processing temperatures higher or close to 200 °C, such as polyamides and polyesters [1,3].

However, magnesium hydroxide used as flame retardant filler is more expensive than ATH. The high purity of magnesium hydroxide together with the costs associated with the optimisation of its particle size and shape in order to improve its effectiveness in polymeric matrices are the main factors responsible for its high price. Low-grade magnesium hydroxide (LG-MH), an industrial by-product obtained in the calcination of magnesia, has been used by some researchers as flame retardant filler in polymeric materials with very promising results [7,8]. As LG-MH costs less than pure magnesium hydroxide, it can be used as cheap filler in materials commonly used without flame retardant for economic reasons.

The endothermic decomposition of LG-MH is also relevant to the formulation of mortars for passive fire protection [9,10]. In this case, LG-MH acts as an aggregate that delays the advance of temperatures in case of fire, which means these mortars can be used to protect building structures from fire [11–13]. The use of low cost materials and/or by-products leads to a combination of an economical and sustainable solution for passive fire protection.

Since LG-MH consists of several hydroxide and carbonate phases and contains several impurities introduced during processing, its thermal behaviour differs substantially from that of pure magnesium hydroxide. In both applications, the thermal properties of the materials formulated with LG-MH differ several respects from pure magnesium hydroxide [7,9]. The presence of an exothermic peak, observed in the analysis of mortars formulated with LG-MH, highlighted the need to study the thermal behaviour of LG-MH. Factors such as its geochemical composition, processing and particle size distribution are strongly related to its thermal behaviour. Hence, the aim of this research was to examine the thermal behaviour of LG-MH, in order to find more efficient formulations of mortars and

* Corresponding author. Tel.: +34 93 403 7244; fax: +34 93 403 5438.
E-mail address: chimenos@ub.edu (J.M. Chimenos).

0040-6031/$ – see front matter © 2010 Elsevier B.V. All rights reserved.
doi:10.1016/j.tca.2010.12.018

know to establish the temperature interval for passive fire protection.

2. Experimental

2.1. Materials

The LG-MH used in this study is produced and sold by Magnesitas Navarras During the calcination of natural magnesite in a horizontal rotary kiln at 1100 °C to obtain caustic calcined magnesia, magnesium oxide powder is collected in the fabric filters and cyclones of the air pollution control system. The flue-dust collected is stockpiled, tempered with water, and then weathered outdoors for a long period, resulting in the hydration of magnesium oxide. The final product is a LG-MH called Envimag®.

To carry out the physicochemical characterization, LG-MH was analysed by X-ray fluorescence (XRF) using a Philips PW2400 X-ray sequential spectrophotometer to elucidate the major and minor components. X-ray diffraction pattern was performed in a Bragg-Brentano Siemens D-500 powder diffractometer with Cu Kα radiation to obtain information about the crystalline phases. Bulk density was measured with helium pycnometer and the specific surface by the BET single point method with a Micrometrics Tristar 3000 porosimeter. Finally, particle size distribution was determined by light scattering with a Beckman Coulter LS13 320 apparatus.

2.2. Thermal analysis

A TA Instruments SDT Q600 Simultaneous TGA-DSC was employed to evaluate LG-MH thermal decomposition by means of thermogravimetric analysis (TGA). TGA were performed in two different atmospheres: air and nitrogen (N_2), with a continuous heating rate of 10 °C min^{-1}. For all experiments, 30.0 ± 0.5 mg of LG-MH was used and the flow rate was 100 mL min^{-1} over the sample. Each sample was previously stabilised at 50 °C and heated at the defined heating rate up to 1000 °C or 1400 °C. Moreover, differential scanning calorimetry (DSC) was simultaneously determined by the same thermal decomposition experiments to measure the heat flow associated with thermal decomposition. In all DSC curves the heat flow signal was corrected by taking into account the sample's mass at each temperature. The Universal V4.7A software of TA instruments was used for thermal analysis interpretation.

In situ high-temperature X-ray diffraction (XRD) patterns were collected at 125, 250, 375 and 500 °C, and between 500 and 800 °C at intervals of 20 °C with a Bragg-Brentano Siemens D-500 powder diffractometer provided with an Anton Paar HTK 1200N high temperature chamber. The sample properly milled was heated in an air atmosphere at 10 °C min^{-1} and then allowed to stabilise for 5 min at the required temperature before its XRD was recorded.

To establish the parameters of the thermal decomposition of some natural carbonates contained in the LG-MH, a sample of the ore feeding the kilns of caustic magnesia was also studied and characterised. Also studied was the decomposition of petcoke used as a fuel during the industrial process of calcinations of the natural magnesite.

3. Results and discussion

The diffraction pattern at room temperature of LG-MH (Fig. 1) shows brucite –$Mg(OH)_2$– as the major phase and unburned magnesite –$MgCO_3$– as a minor one, along with dolomite –$MgCO_3{\cdot}CaCO_3$– and quartz –SiO_2–, which occur in natural magnesite. The calcite (or aragonite) –$CaCO_3$– present in natural magnesite, in addition to that generated during the tempering and weathering process of stockpiled flue-dust, is also present in a lower extent.

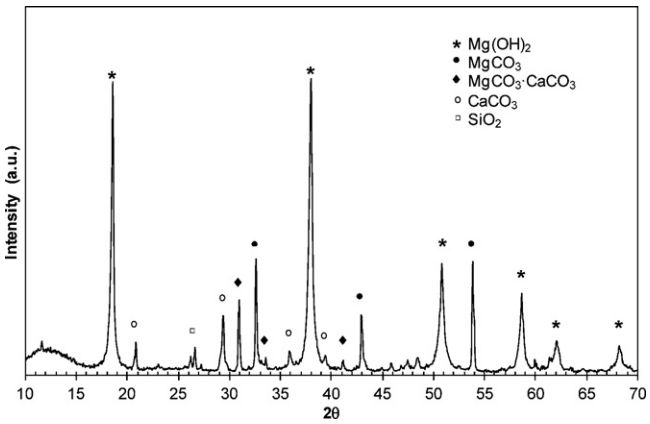

Fig. 1. X-ray pattern of LG-MH.

Table 1 shows the chemical composition and the physical parameters of the LG-MH used in this study. The results obtained by FRX corroborate those obtained by DRX, taking into account that the percentage of CaO comes from both the dolomite and calcite. LG-MH has about 50% of MgO, which means that it may have about 72% of $Mg(OH)_2$ if one considers that all the MgO is hydrated to form brucite. Actually this percentage of MgO hydrolysed is lower because of the presence of magnesite and dolomite, previously determined by means of DRX. As can be seen in Table 1, LG-MH exhibits a mean particle size below 100 μm, which makes it suitable for use both as fine aggregate in mortars and flame retardant in polymer compounding (d_{50} < 100 μm), which can be used as it is in the mortar formulation or as a filler in the plastic compounding [7,9].

Fig. 2 shows the thermal decomposition up to 1000 °C of LG-MH in air atmosphere. The TG curve shows a total mass loss of about 33.3%, which is close to the LOI determined by FRX (see Table 1). This total mass loss takes place in four consecutive stages. The mass loss below 200 °C corresponds to the release of the moisture content and water absorbed into the pores of the LG-MH. The second stage corresponds to the thermal dehydroxylation of $Mg(OH)_2$ (Eq. (1)) with water vapour release in the range of 241–484 °C. The DTG curve shows for this stage a peak centred on 400 °C, which is close to these determined by other authors [3,14]. The mass loss in the range of 484–645 °C is due to the decarbonation of $MgCO_3$ (Eq. (2)).

Table 1
Physicochemical characterization of LG-MH.

	LG-MH	Ore feeding
MgO (%)	49.01	41.45
CaO (%)	6.69	5.07
SiO_2 (%)	2.63	2.50
Fe_2O_3 (%)	2.06	1.50
SO_3 (%)	2.80	0.17
Al_2O_3 (%)	0.35	0.25
MnO (%)	0.11	
P_2O_5 (%)	0.08	
V_2O_5	0.14	
K_2O (%)	0.10	
TiO_2 (%)	0.02	
LOI (1100 °C) (%)	32.89	49.23
Density (g cm^{-3})	2.44	
Specific surface (m^2 g^{-1})	22.11	
d_{90} (μm)	219	
d_{50} (μm)	88	
d_{10} (μm)	17	

LOI: loss of ignition. d_x: accumulated fraction lower than particle size.

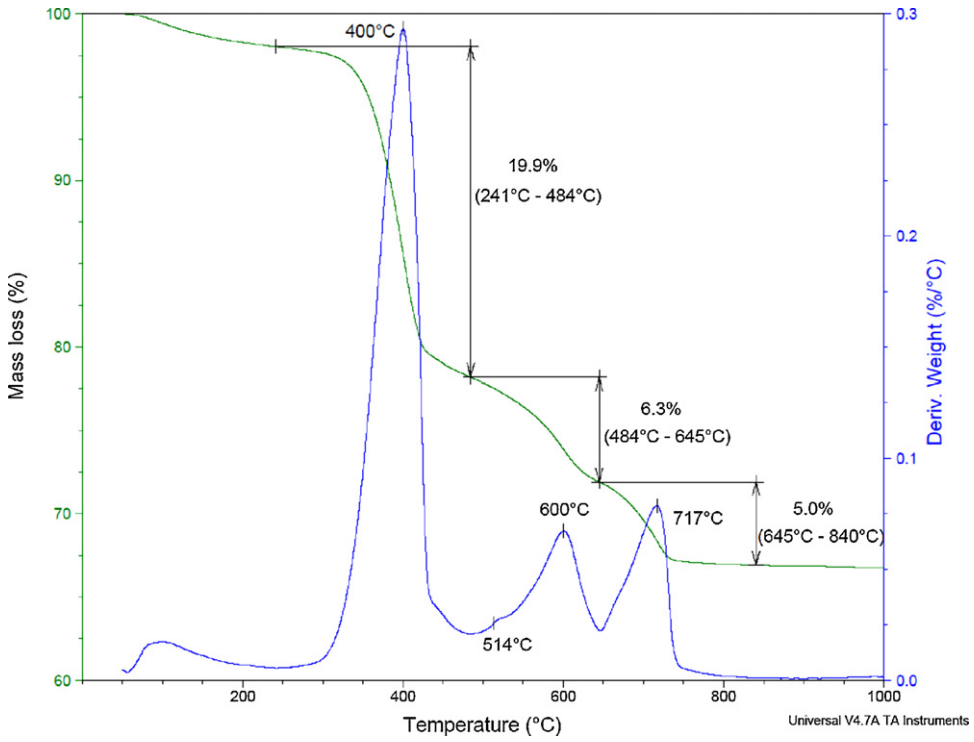

Fig. 2. TG-DTG curves of thermal decomposition of LG-MH up to 1000 °C in air atmosphere.

However, in this temperature range, the derivate of the TGA curve (DTG) shows two peaks; a small peak centred on 514 °C and another one centred on 600 °C. The fourth stage in the range of 645–840 °C is attributed to the thermal decomposition of $MgCO_3{\cdot}CaCO_3$. The thermal decomposition of dolomite in air atmosphere takes place in only one step (Eq. (3)) as can be observed in the DTG curve, where a single peak centred on 717 °C was determined. Nevertheless, it is surprising to observe that the TGA–DTG curves does not show the mass loss corresponding to the $CaCO_3$ determined previously by DRX (see Fig. 1).

$$Mg(OH)_{2\,(s)} \xrightarrow{T=241-484\,^{\circ}C} MgO_{(s)} + H_2O_{(g)} \quad (1)$$

$$MgCO_{3\,(s)} \xrightarrow{T=484-645\,^{\circ}C} MgO_{(s)} + CO_{2(g)} \quad (2)$$

$$MgCa(CO_3)_{2\,(s)} \xrightarrow{T=645-898\,^{\circ}C} MgO_{(s)} + CaO_{(s)} + 2CO_{2\,(g)} \quad (3)$$

The thermal decompositions of dehydroxylation and decarbonation are both endothermic reactions. Hence, it was expected that the DSC curve would show only the endothermic peaks at temperatures close to those determined previously in the DTG analysis. However, the DSC curve of the thermal decomposition of LG-MH in air atmosphere (Fig. 3) also shows an exothermic peak at 600 °C. The first DSC peak at 407 °C is due to the dehydroxylation of $Mg(OH)_2$ with an associated endothermic heat flow of about 722 J g^{-1}. Nevertheless, the DSC curve shows an exothermic peak instead of the second expected endothermic peak corresponding to the decarbonation of $MgCO_3$. This exothermic peak, with an integrated heat flow of 305 J g^{-1}, explains the exothermic behaviour observed at this temperature range in the mortars formulated with LG-MH as aggregate [9]. Finally, the DSC curve shows a last endothermic peak at 722 °C corresponding to the decarbonation of dolomite with an associated heat flow of about 213 J g^{-1}.

Fig. 4 shows the thermal decomposition up to 1000 °C of LG-MH in N_2 atmosphere. Great differences can be seen depending on the gas flow. First, the TGA curve obtained using N_2 exhibits a total mass loss of 34.7%, which is about 1.4% greater than that obtained with air atmosphere. The mass loss associated with thermal dehydroxylation of $Mg(OH)_2$ (19.1%), with a DTG peak centred on 410 °C, is very similar to that determined with air as gas flow. Decarbonation of $MgCO_3$ (588 °C) appears 12 °C earlier than when using air atmosphere, but thermal decomposition of $MgCO_3{\cdot}CaCO_3$ (734 °C) occurs 17 °C later in nitrogen atmosphere. Once again a small peak is observed in the temperature range associated with decarbonation of $MgCO_3$ (475–647 °C), in this case centred on 521 °C. In addition, the TGA curve using N_2 has an additional mass loss of 2.9% in the 805–990 °C range. This mass loss may be attributed to the decarbonation of $CaCO_3$, which was previously identified by DRX in LG-MH (see Fig. 1), but was not identified in the thermal analysis performed in air.

The comparison of DSC obtained in the thermal decomposition of LG-MH at different gas flow is shown in Fig. 5. As seen in the figure, the peaks determined in the DSC curve obtained in N_2 atmosphere are displaced to higher temperatures, according to DTG curves observed above. Despite this, the endothermic dehydroxylation of $Mg(OH)_2$ and decarbonation of $MgCO_3{\cdot}CaCO_3$ are very similar in both air and N_2 gas flows. Nevertheless, unlike the curve obtained in air atmosphere that shows a high exothermic peak, the DSC curve obtained in N_2 shows an endothermic peak at 604 °C that can be attributed to the decarbonation of $MgCO_3$. Moreover, in the DSC curve using N_2 gas, a small endothermic peak at 526 °C can be observed. This peak can be related to the small DTG peak shown at 521 °C. In addition, an endothermic peak at 928 °C, attributed to decarbonation of $CaCO_3$ appears in the N_2 gas flow.

The simultaneous TG-DSC up to 1000 °C in air atmosphere from the ore feeding the kilns of caustic magnesia was also studied. The DTG and endothermic DSC peaks corresponding to the decarbonation of $MgCO_3$ and $MgCO_3{\cdot}CaCO_3$ are in the same temperature range as those obtained from LG-MH. However, no exothermic peak was observed in the thermal decomposition of the ore. This means that the exothermic peak observed in the thermal decomposition

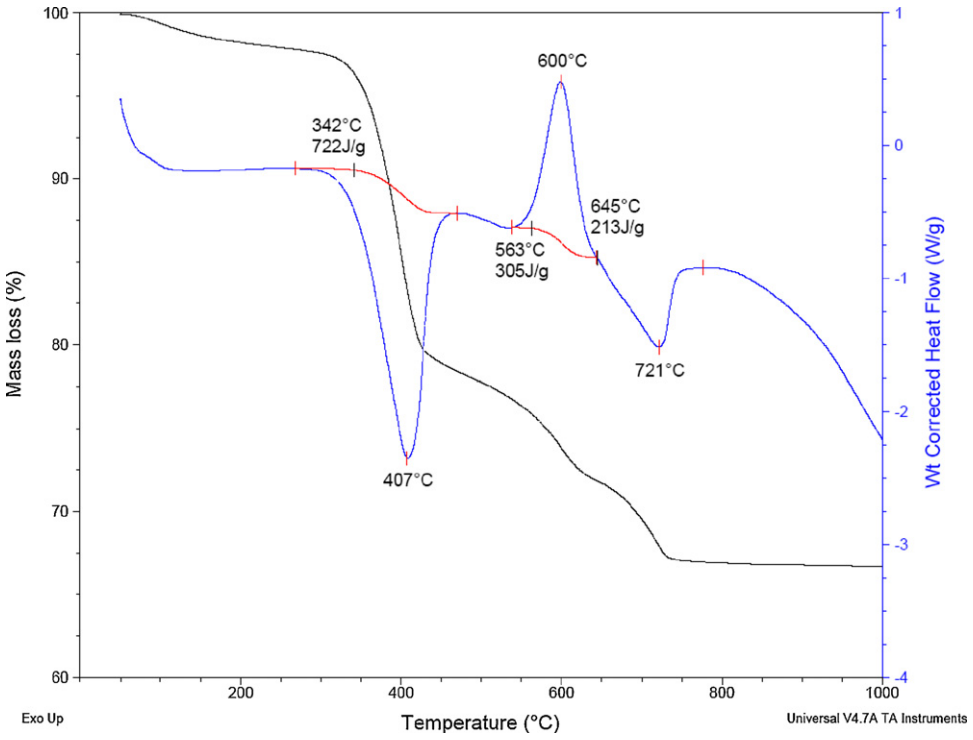

Fig. 3. DSC curve of thermal decomposition of LG-MH up to 1000 °C in air atmosphere.

of LG-MH (Fig. 3) may be related to some product or by-product generated during the combustion process of the natural magnesite in the industrial kilns.

Although the rotary kiln can be fired using gas, oil or solid fuel, the petcoke is the cheaper fuel and the most worldwide used. Taking into account this fact, it is possible that the observed exothermic reaction may be due to the combustion of the petcoke particles collected with the particles of LG-MH; or some by-products generated during the pyrolysis of petcoke. To elucidate this assumption, the thermal decomposition up to 1200 °C of a sample of petcoke in both air and N_2 atmospheres was studied (Fig. 6). As expected, there is a great difference in the thermal decomposition of petcoke as a function of the gas flow used. In both air and N_2 atmosphere the mass loss occurs in a single stage, with the DTG peak centred at

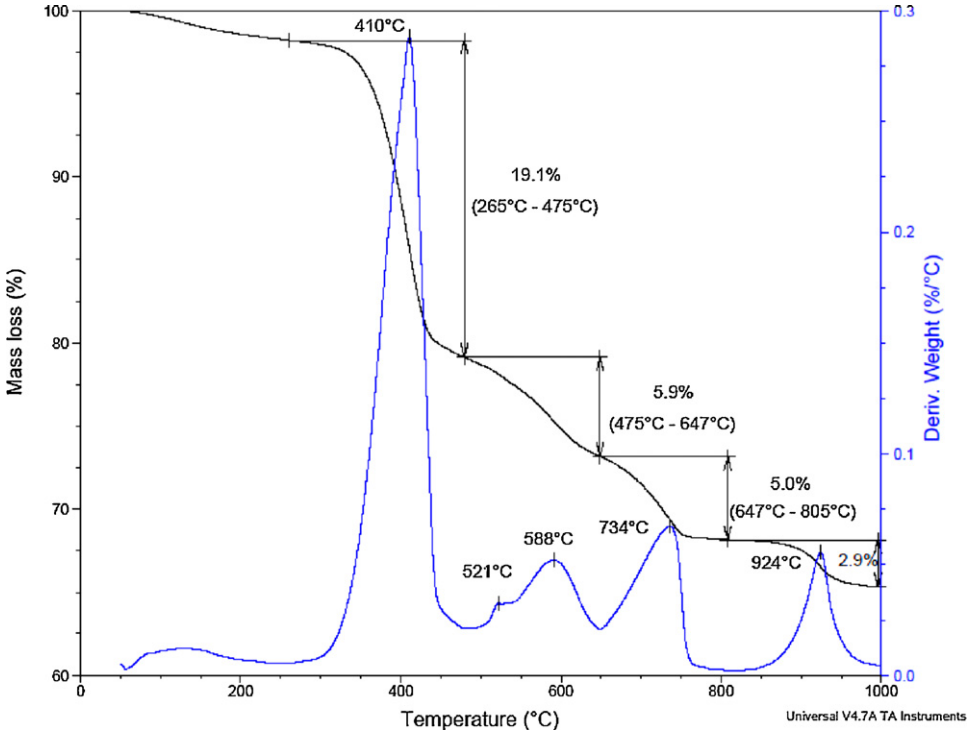

Fig. 4. TG-DTG curves of thermal decomposition of LG-MH up to 1000 °C in N_2 atmosphere.

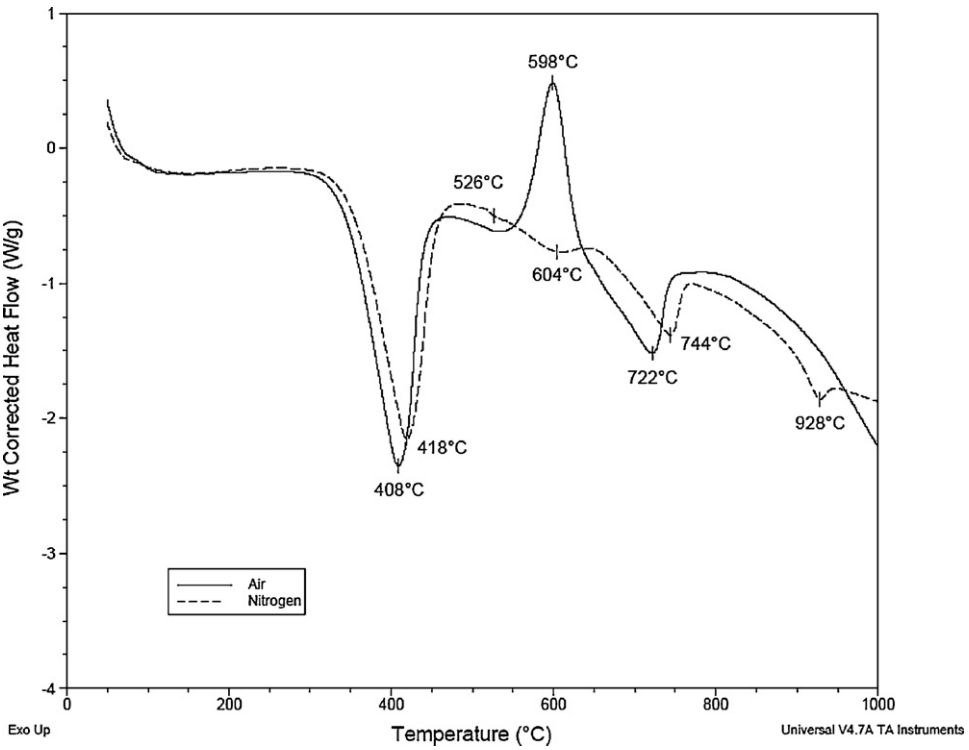

Fig. 5. Comparison of DSC curves of thermal decomposition of LG-MH up to 1000 °C in N_2 and air atmospheres.

516 °C and 528 °C, respectively. The mass loss using air atmosphere is close to 100% because of the total combustion of the petcoke, whereas only 14% was determined with N_2 as a gas flow. This mass loss when the N_2 gas was used is due to the loss of the volatile matter during the pyrolysis of petcoke, with the char or other non volatile matter (tars) remaining. This fact can be corroborated in the DSC curves. Thus, whereas the DSC curve in air atmosphere shows a large exothermic peak centred on 540 °C, the variation in the DSC curve using N_2 is negligible. According to this, the presence of petcoke particles, or char and tars generated during the pyrolysis of this, may explain the exothermic peak determined in the thermal decomposition of LG-MH at 600 °C (see Fig. 3). The differences between the temperatures determined in the two exothermic peaks may be due to the combustion of different substances, i.e.

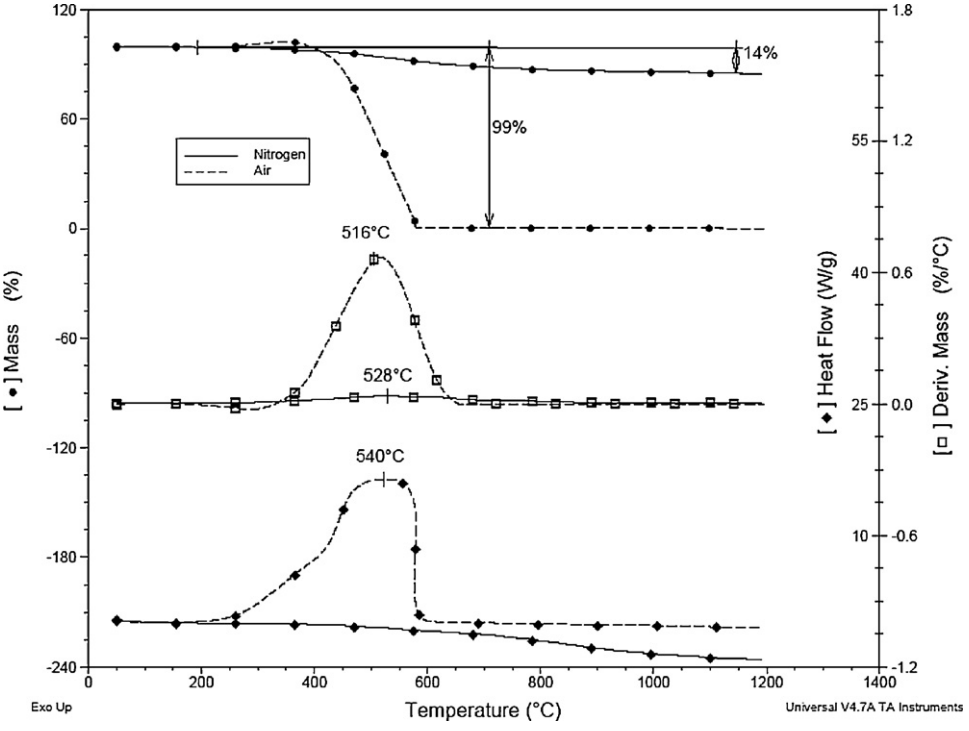

Fig. 6. TG-DTG–DSC curves of thermal decomposition of petcoke up to 1200 °C in air and N_2 atmospheres.

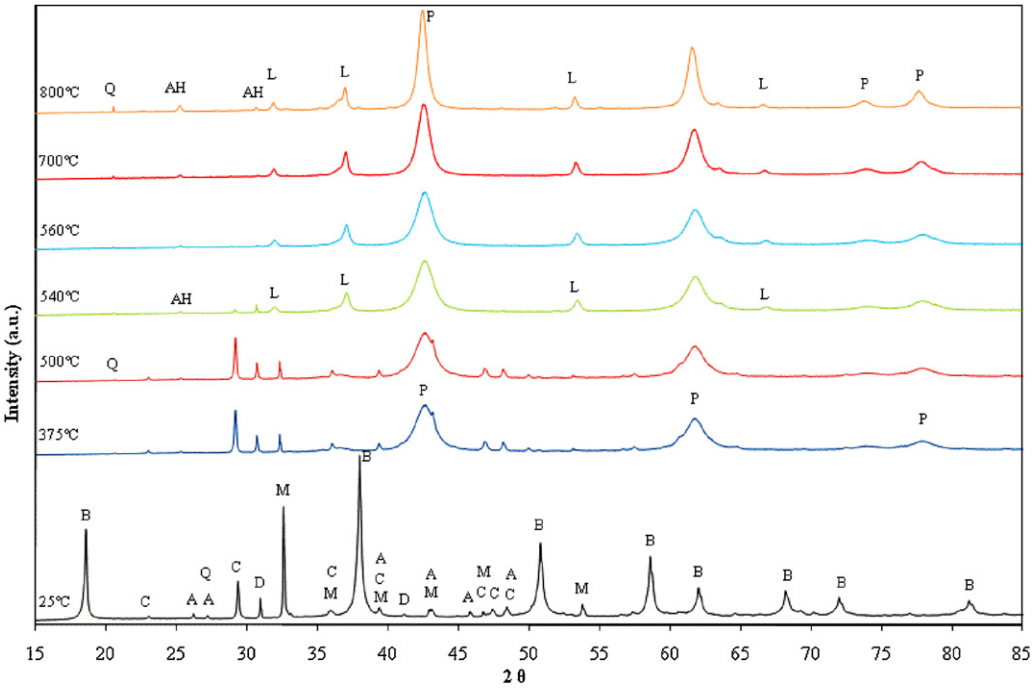

Fig. 7. XRD pattern of LG-MH at different temperatures. Brucite ($Mg(OH)_2$, B), magnesite ($MgCO_3$, M), dolomite ($MgCO_3{\cdot}CaCO_3$, D), calcite ($CaCO_3$, C), aragonite ($CaCO_3$, A), quartz (SiO_2, Q), periclase (MgO, P), lime (CaO, L) and anhydrite ($CaSO_4$, AH).

whereas the exothermic peak in Fig. 6 corresponds to the combustion of the petcoke used by Magnesitas Navarras in the industrial combustion of natural magnesite, the exothermic peak in Fig. 3 may be due to the combustion of char or tars generated by the pyrolysis of this petcoke during the industrial process.

To remove the petcoke or char particles collected with LG-MH a solvent extraction of a sample was carried out. The extraction was made according to the Soxhlet's procedure using hexane as organic solvent. After solvent extraction, thermal analysis of the sample was conducted. As expected, the TGA–DTG curves showed the same stages and the same peaks as those determined for the sample without the extraction (Fig. 2). However, the DSC curve shows again the exothermic peak attributed to petcoke combustion, with associated heat of the same order of magnitude as that determined previously (Fig. 3). This indicates clearly that solvent extraction is not an effective method for removing petcoke or char,

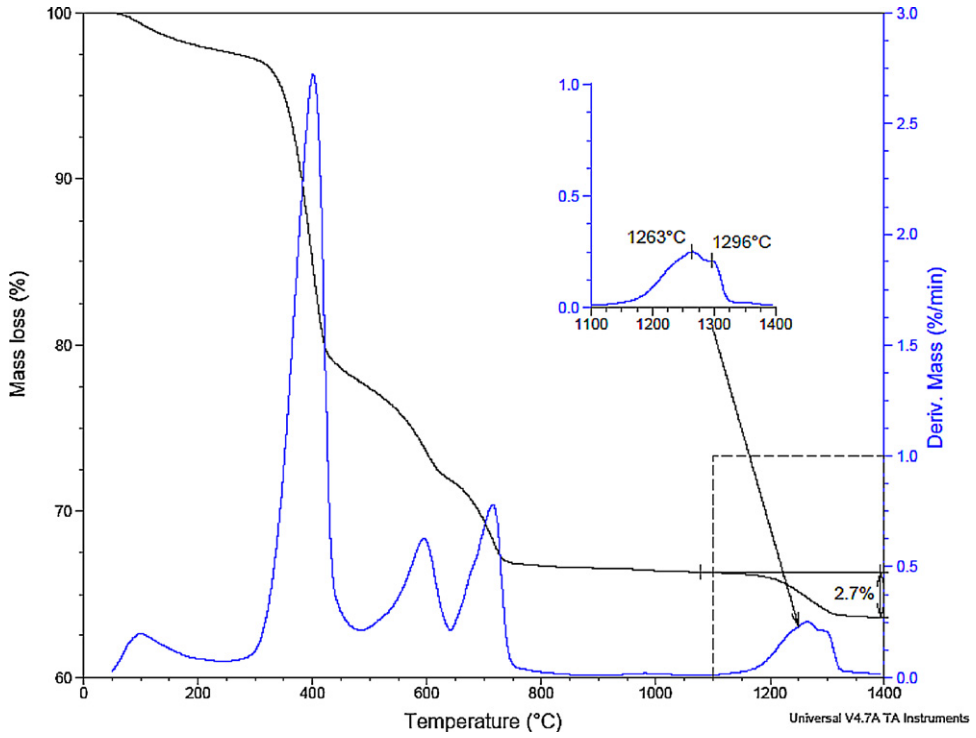

Fig. 8. TG-DTG curves of thermal decomposition of LG-MH up to 1400 °C in air atmosphere.

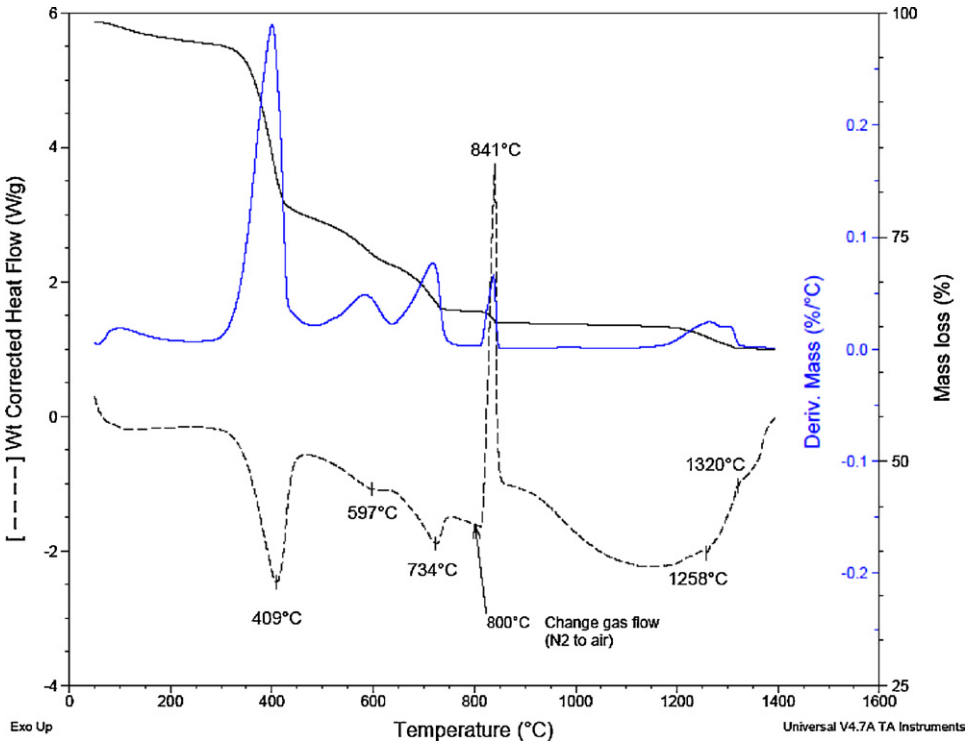

Fig. 9. TG-DTG–DSC curves of thermal decomposition of LG-MH up to 1400 °C. Change of the gas flow control at 800 °C (N_2 to air).

which is consistent with the results obtained by other author using a wide variety of organic solvents [14].

Fig. 7 depicts the powder X-ray diffraction patterns of a LG-MH sample at different temperatures. In the figure, only the XRD patterns obtained at significant temperatures are shown. However, as each XRD pattern was collected using an isothermal procedure (see Section 2.2.), the crystalline phases determined at each temperature were not necessary the same as those established in the TGA–DTG curves. For example, the $Mg(OH)_2$ and $MgCO_3{\cdot}CaCO_3$ were not identified by XRD at 375 °C and 560 °C, respectively. The presence should be noted of anhydrite ($CaSO_4$) from 540 °C, whose main peak appears at $2\theta = 25.5°$ and minor peaks appear at $2\theta = 30.3°$, 36.0°, 39.6° and 51.1°, coinciding with the extinction of $CaCO_3$.

The sulphation of $CaCO_3$ has been widely studied by other authors [15–17] as a conventional and economically feasible method for removing sulphur dioxide (SO_2) from various industrial processes. If the decarbonation of $CaCO_3$ to form CaO takes place before reacting with SO_2, the process is often called an indirect sulphation reaction; whereas if the decarbonation of $CaCO_3$ does not take place the SO_2 may react directly with limestone and the process is called direct sulphation reaction and is expressed according to the following reactions [18]:

$$CaCO_{3(s)} + SO_{2(g)} + \tfrac{1}{2}O_{2(g)} \rightarrow CaSO_{4(s)} + CO_{2(g)} \quad (4)$$

The chemistry involved in Eq. (4) needs an excess of O_2 or the presence of some catalysts, then the SO_2 can be converted to SO_3 [16]. Furthermore, the presence of $MgCO_3$ in relatively high concentrations such as in LG-MH, significantly promote the sulphation reaction [19].

In the thermal decomposition of LG-MH, the direct sulphation of $CaCO_3$ to form $CaSO_4$ would explain the differences in mass loss obtained as a function of the gas flow used. Thus, whereas in N_2 atmosphere the thermal decomposition of LG-MH involves the decarbonation of $CaCO_3$ (see Fig. 4) with a DTG peak centred at 924 °C, the anhydrite formed in air atmosphere does not decompose below 1000 °C. To study the thermal decomposition of the anhydrite generated, a TGA up to 1400 °C (Fig. 8) was performed. The TGA curve shows a decomposition stage in the range of 1150–1350 °C with a mass loss of 2.7% that can be related to the conversion of $CaSO_4$ to CaO with the loss of sulphur trioxide (SO_3) gas. The DTG curve shows two peaks (1263 and 1296 °C) reported by other authors during the decomposition of calcium sulphate [20–22]. The first peak is related to the decomposition of α-$CaSO_4$; and the second one to the eutectic mixture of $CaSO_4$ and CaO. This percentage of SO_3 is very close to the amount determined by XRF (see Table 1), with the total content of sulphur in LG-MH at around 1%. However, given the percentage of $CaCO_3$ (6.6%), calculated from the mass loss of LG-MH in N_2 atmosphere (see Fig. 4), it can be concluded that the amount of sulphur is not enough to sulphate all calcite contained in the by-product. Under this assumption, other metal oxide acids formed during combustion of petroleum coke react with calcium carbonate to form the corresponding calcium oxyanions, e.g. calcium vanadate or calcium nitrate [23,24].

However, the TGA–DTG curves obtained up to 1400 °C in N_2 atmosphere, show no mass loss in the 1000–1400 °C range, which confirms that $CaSO_4$ only form in air atmosphere [16,17]. Nevertheless, the change of gas flow and the introduction of air at 800 °C during the thermal decomposition of LG-MH in N_2 atmosphere (Fig. 9) show a narrow exothermic peak, which is related to the combustion of char and non volatile matter generated during the pyrolysis of petcoke and still remaining with the LG-MH particles. At this temperature, the SO_3 formed in the combustion reacts with $CaCO_3$ to form anhydrite, which decomposes later.

4. Conclusions

The thermal analysis of LG-MH shows an important mass loss due to the endothermic reactions that take place during its decomposition. This thermal behaviour means that this by-product could be used as filler in flame retardant polymers or as aggregate in mortars used for passive fire protection.

However, it has been also determined that the thermal decomposition of LG-MH in air atmosphere presents an exothermic peak due to the presence of small amounts of petcoke or char collected with LG-MH. A large exothermic heat is released due to the desulphurisation of petcoke or char under combustion conditions. The sulphur trioxide generated with the excess of oxygen reacts directly with the $CaCO_3$ to produce $CaSO_4$, which decomposes at temperatures above 1150 °C. These events were not observed in the thermal decomposition of LG-MH in N_2 atmosphere because the desulphurisation of petcoke (or char) and direct sulphation of $CaCO_3$ do not take place. In this case, the thermal decomposition of $CaCO_3$ was observed.

The exothermic peak has no impact on the effectiveness of LG-MH used as flame-retardant filler, because the petcoke or char combustion occurs at temperatures greater than the ignition temperature of most polymers. However, the effectiveness of LG-MH used as aggregate in mortars for passive fire protection may be affected by the combustion heat of the petcoke or char collected with the LG-MH. Since the petcoke or char particles cannot be removed by solvent extraction processes, the exothermic heat could be compensated for by adding other aggregates, whose endothermic decomposition takes place in the same temperature range, e.g. natural magnesite.

Acknowledgements

The authors would like to thank Magnesitas Navarras S.A., the Spanish Ministry of Science and Innovation (project FIS2009-13360-C03-03) and the Generalitat of Catalonia (project 2009SGR878) for supporting and financing this research project.

References

[1] R.N. Rothon, Particulate-Filled Polymer Composites, second ed., Rapra Technology Limited, Shrewsbury, UK, 2003.
[2] R.N. Rothon, P.R. Hornsby, Flame retardant effects of magnesium hydroxide, Polym. Degrad. Stabil. 54 (1996) 383–385.
[3] J. Zhang, X. Wang, F. Zhang, A.R. Horrocks, Estimation of heat release rate for polymer–filler composites by cone calorimetry, Polym. Test. 23 (2004) 225–230.
[4] M. Sain, S.H. Park, F. Suhara, S. Law, Flame retardant and mechanical properties of natural fibre–PP composites containing magnesium hydroxide, Polym. Degrad. Stabil. 83 (2004) 363–367.
[5] D.T.Y. Chen, P.H. Fong, Thermal analysis of magnesium hydroxide, J. Thermal. Anal. 12 (1977) 5–13.
[6] L.A. Hollingbery, T.R. Hull, The thermal decomposition of huntite and hydromagnesite—a review, Thermochim. Acta 509 (2010) 1–11.
[7] A.I. Fernández, L. Haurie, J. Formosa, J.M. Chimenos, M. Antunes, J.I. Velasco, Characterization of poly(ethylene-co-vinyl acetate) (EVA) filled with low grade magnesium hydroxide, Polym. Degrad. Stabil. 94 (2009) 57–60.
[8] J.M. Chimenos, A.I. Fernández, F. Espiell, M. Segarra, J. Formosa, J.I. Velasco, Magnesium mineral composition for use in polymeric matrices, ES 2 288 421 B1. (2006) (written in Spanish).
[9] J. Formosa, L. Haurie, J.M. Chimenos, A.M. Lacasta, J.R. Rosell, Comparative study of magnesium by-products and vermiculite formulations to obtain fire resistant mortars, Mater. Sci. Forum 587–588 (2008) 898–902.
[10] J. Formosa, J.M. Chimenos, A.M. Lacasta, L. Haurie, J.R. Rosell, Novel fire-proof mortars formulated with magnesium by-products, Cement Concrete Res. 41 (2011) 191–196.
[11] L.F. Vilches, C. Fernández-Pereira, J. Olivares del Valle, M.A. Rodríguez-Piñero, J. Vale, Development of new fire-proof products made from coal fly ash: the CEFYR project, J. Chem. Technol. Biotechnol. 77 (2002) 361–366.
[12] L.F. Vilches, C. Fernández-Pereira, J. Olivares del Valle, J. Vale, Recycling potential of coal fly ash and titanium waste as new fireproof products, Chem. Eng. J. 95 (2003) 155–161.
[13] L.F. Vilches, C. Leiva, J. Vale, J. Olivares, C. Fernández-Pereira, Fire resistance characteristics of plates containing a high biomass-ash proportion, Ind. Eng. Chem. Res. 46 (2007) 4824–4829.
[14] H. Al-Haj-Ibrahim, B.I. Morsi, Desulfurization of petroleum cokes: a review, Ind. Eng. Chem. Res. 31 (1992) 1840–1848.
[15] K. Nahdi, F. Rouquerol, M.T. Ayadi, Mg(OH)2 dehydroxilation: A kinetic study by controlled rate thermal analysis (CRTA), Solid State Sci. 11 (2009) 1028–1034.
[16] M.J.H. Snow, J.P. Longwell, A.F. Sarofim, Direct sulfation of calcium carbonate, Ind. Eng. Chem. Res. 27 (1988) 268–273.
[17] M.R. Hajaligol, J.P. Longwell, A.F. Sarofim, Analysis and modeling of the direct sulfation of $CaCO_3$, Ind. Eng. Chem. Res. 27 (1988) 2203–2210.
[18] G. Hu, K. Dam-Johansen, S. Wedel, J.P. Hansen, Review of the direct sulfation reaction of limestone, Prog. Energy Combust. Sci. 32 (2006) 386–407.
[19] E. Alvarez, J.F. González, High pressure thermogravimetric analysis of the direct sulfation of Spanish calcium-based sorbents, Fuel 78 (1999) 341–348.
[20] S. Arvelakis, P.A. Jensen, K. Dam-Johanses, Simultaneous thermal analysis (STA) on ash from high-alkali biomass, Energy Fuels 18 (2004) 1066–1076.
[21] Netzch. Technical Information. Building Materials. Gypsum (Calcium Sulfate Dihydrate). www.netzsch-thermal-analysis.com/download/009-2006-STA409PC-Inorganics-BuildingMaterials-Gypsum_42.pdf (revised in September 2010).
[22] Y. Pelovski, V. Petkova, Mechanism and kinetics of inorganic sulphates decomposition, J. Thermal Anal. 49 (1997) 1227–1241.
[23] E.J. Anthony, R.E. Talbot, L. Jia, D.L. Granatstein, Agglomeration and fouling in three industrial petroleum coke-fired CFBC boilers due to carbonation and sulfation, Energy Fuels 14 (2000) 1021–1027.
[24] C. Ettarha, A.K. Galwey, Thermal analysis of anhydrous mixtures of calcium nitrate and selected metal oxides, Thermochim. Acta 61 (1995) 125–139.